Carbon 159 (2020): 303-310

DOI: https://doi.org/10.1016/j.carbon.2019.12.053

Direct Covalent Immobilization of new Nitrogen-doped Carbon Nanodots by Electrografting for Sensing Applications

Cristina Gutiérrez-Sánchez[1], Mónica Mediavilla[1], Tamara Guerrero-Esteban[1], Mónica Revenga-Parra[1,2,3], Félix Pariente[1,2,3] and Encarnación Lorenzo[1,2,3*]

[1]Departamento de Química Analítica y Análisis Instrumental, Universidad Autónoma de Madrid, Ciudad Universitaria de Cantoblanco, 28049 Madrid, Spain.

[2]Institute for Advanced Research in Chemical Sciences (IAdChem), Universidad Autónoma de Madrid, Ciudad Universitaria de Cantoblanco, 28049, Madrid, Spain.

[3]IMDEA-Nanociencia, Ciudad Universitaria de Cantoblanco, 28049, Madrid, Spain

*Corresponding author. Tel: +34 91 4974488. E-mail: encarnacion.lorenzo@uam.es (Encarnación Lorenzo)

ABSTRACT

This paper reports a facile strategy to covalently immobilize nanosized carbon dots (CD) onto carbon conductive surfaces for sensing applications. The carbon nanodots designed with surface amine groups (N-CD) can be electrografted onto carbon electrodes and, thus, easily covalently immobilized on these conductive surfaces. They have been synthetized by a carbonization method microwave-assisted using preselected low cost and biocompatible precursors, such as D-fructose as primary carbon source and urea as N-donor reagent to obtain peripheral enriched nitrogen CD. The synthetized nanomaterial has been characterized by different techniques, that confirm the presence of size-regular amorphous structures with blue fluorescence when are irradiated with UV light. The highly stable immobilization of N-CD onto the electrode surfaces by electrografting provides hybrid electrodes with greater relative surface area and improved electron transfer properties, demonstrating to be a great promise for electrochemical sensing. Because of its good electrical conductivity, electrical properties, abundant edges sites and high catalytic activity, N-CD immobilized on carbon electrodes efficient amplify the electrochemiluminiscence (ECL) signal from the luminophore $[Ru(bpy)_3]^{2+}$ in a taurine sensor. A linear concentration range from 126 to 1000 µM, a sensitivity of $7.40x10^{-4}$ μM^{-1} and a detection limit of 37.8 µM were determined for the taurine sensor.

KEYWORDS

Aryldiazonium salts, carbon nanodots, electrografting, electrochemilumiscence.

1. Introduction

In recent years a wide variety of carbon nanomaterials have been described in the literature and their preparation, structure, properties and applications have been extensively studied. These studies and the wide ranging properties of such material have focused the interest of researchers during the last decade [1, 2]. More recently, carbon nanodots (CD) have emerged as a new type of carbon-based nanostructure showing very low dimensionality with a diameter between 5-15 nm and characteristic photoluminiscent properties [3]. CD can be prepared following several top-down and bottom-up methodologies such as electrochemical etching [4, 5], pyrolysis [6], hydrothermal synthesis [7] and microwave-assisted synthesis [8]. Among them, the bottom-up microwave-assisted methods have become very popular because it is a low-cost procedure, uses very common starting materials and the final product can be achieved in one single step in a short time. CD obtained from this approach are in general stable, soluble in aqueous medium and present low toxicity. These properties make them biocompatible, allowing to be used in a large number of biological applications [9-12]. In addition, the bottom-up approach has shown that the choice of the starting materials is critical to obtain CD with a great structural variety. For example, heteroatoms can be introduced during the synthesis by using nitrogen-rich precursors. In general, CD consist of a compact nucleus formed by condensed aromatic rings of sp^2 carbon and a crust in which there are sp^3 carbons modified with a great variety of functional groups that provide these nanostructures their different chemical and optical properties [11]. Among them, one of the most relevant is their photoluminescence (PL), with high quantum yields that can be modulated by varying the excitation wavelengths [13, 14].

The photoluminescent CD properties are difficult to explain due to the great structural diversity exhibited by these nanomaterials. The wide range of fluorescent emissions observed in CD dispersions can be explained by quantum-size effects [15] or by the presence of different types of functional groups located at the zig-zag edges surrounding the CD core [16-18]. All these

combined factors can affect the HOMO, LUMO and band gap of the CD, enabling the deliberate modulation of the photoluminescent characteristics of these nanostructures. This confirms their donor/acceptor CD properties. In this context, CD are more versatile than traditional quantum dots based on semiconductors [13, 19].

Moreover, a significant alteration of the electronic, chemical and interfacial CD properties can be achieved by doping their surface with heteroatoms. In this way, there are precedents with other carbon-based nanomaterials. It has been reported that the modification of carbon nanotubes with nitrogen-containing functional groups improves their electrocatalytic properties for the reduction of molecular oxygen [20, 21]. In a similar way, doping graphene with nitrogen heteroatom modulates their band gap so that it can be applied in electrocatalysis [22], semiconductor devices [23], design of supercapacitors [24] and in biosensing with optical and electrochemical detection [25]. In this sense, synthesis of CD doped with nitrogen containing functional groups (N-CD) allows to obtain nanostructures with tuneable luminescent properties [26, 27]. In these reports, the N-CD synthesis involves a precursor that acts as a carbon source and a second precursor that provides the nitrogen source [28, 29]. The C/N ratio is used to establish a relationship between the properties of the nanostructure and the nitrogen content on its surface.

CD show unique intrinsic properties, such as a strong ability for electron transfer, abundant edge sites, high catalytic activity and large specific surface area due to the small size, which make CD advantageous for electrochemical sensing [11]. However, while CD have gained tremendous attention for their unique properties, as far as we know, no studies of direct covalently immobilized CD on electrode surface have been reported. The coupling of carbon nanodots with electrodes to produce conductive nanostructured hybrid materials is highly interesting for electrochemical (bio)sensor development. Enabling such an application will require the appropriate strategy of surface immobilization of the CD. Specifically, such an immobilization should be carried out on a matrix that is permeable to the analyte while preventing CD from detaching or losing their properties.

Since Pinson and co-workers described the modification of carbon electrodes by aryldiazonium salts [30], electrochemical reduction of these compounds has been employed for surface functionalization through covalent bonding. It has been demonstrated to be a smart and efficient way to introduce many types of functional groups to decorate a variety of substrates with a reaction time scale from seconds to minutes. However, as far as we know it has been not yet employed to immobilize N-CD on substrates although it can provide a selective and controlled immobilization. Moreover, the possibility to produce modified surfaces based on diazonium chemistry by the application of a potential bias allows for the selective functionalization of closely-spaced microelectrode surfaces.

In the present work, we report a simple synthetic strategy based on fast and controlling microwave heating, to produce nitrogen-doped CD. We selected D-fructose as primary carbon source and urea as N-donor reagent, because both precursors are biocompatible compounds, very common and abundant in the nature, in order to produce CD by a simple, economical and green method. Additionally, urea is a nitrogen-rich precursor, which produce CD peripherally enriched in nitrogen functional groups. These can be employed to functionalize the nanomaterial by post-synthesis reactions. The as-synthetized N-CD optical properties were investigated to establish a relationship between their optical properties and the nitrogen content. As starting point in our strategy, we optimized the stoichiometric ratio of the precursors in order to obtain a nitrogen peripheral enriched final product. The idea was to employ the aromatic amino groups present on N-CD surface to promote diazotization reactions by treatment with sodium nitrite in acidic media. The diazotized N-CD were subsequently electrografted on carbon electrodes resulting in stable coatings that were employed in the design of sensor platforms. As a proof of concept, a taurine sensor based on the ECL properties of the as-prepared N-CD was developed.

2. Experimental

2.1 Chemicals

D-Fructose, urea, taurine and $[Ru(bpy)_3]^{2+}$ were purchased from Sigma-Aldrich. 37% (w/w) hydrochloric acid was obtained from Scharlau and sodium nitrite was purchased from Riedel-de-Haën. Other chemicals used in this work were analytical grade and were used without further purification. A dialysis membrane tubing cut-off in the range of (0.1-0.5) kDa was provided by Spectrum Laboratories. Water purified in a Millipore Milli-Q system was used in all experiments.

2.2 Instrumentation

The electronic transmission microscopy (TEM) measurements were performed in a JEOL JEM 1400 electron microscope. For this purpose, an aqueous solution of N-CD (12.7 mg/mL) was sonicated in an ultrasound bath for 30 min. Then 10 μL of this solution was deposited on a copper grid covered with a thin layer of carbon. It was allowed to dry 15 min and the grid was placed in the sample holder to be observed in the microscope. Elemental analysis was performed with a LECO CHNS-932 elemental analyser. Fourier-transform infrared (FTIR) spectra were recorded from KBr pressed pellets using a Brucker IFS66v spectrometer and XRD polycrystal carried out on a X-pert PRO Theta/2Theta diffractometer from Panalytical. These analyses were made with synthetized N-CD solid samples. Zeta potential were determined in N-CD aqueous solution (0.06 mg/mL) in the presence of 10 mM KNO_3 using a Zetasizer Nano ZS instrument (Malvern Instrument Ltd., Grovewood, Worcestershire, UK). The absorption spectra were measured using UV-1700 series spectrometer (Shimadzu Corp.) and the photoluminescence measurements were carried out in a Cary Eclipse Varian spectrofluorophotometer. UV-visible absorption and fluorescence emission measurements were performed in aqueous solutions using a quartz cell with 1.0 cm optical path. Electrochemical measurements were carried out using a Metrohm Autolab potentiostat PGSTAT 30. Screen-printed graphene electrodes (SPGE), supplied by DropSens-

Metrohm, were used in the electrochemical measurements as integrated electrochemical cells including a carbon ink counter-electrode and a silver pseudo-reference electrode. EIS experiments were performed in 0.1 M acetic acid/acetate buffer (pH=5) containing an equimolar mixture of 10 mM $K_3Fe(CN)_6$/10 mM $K_4Fe(CN)_6$. Impedance measurements were recorded in the range of frequency between 10^5 and $5x10^{-2}$ Hz, with a sinusoidal potential modulation of ±10 mV in amplitude superimposed onto the formal potential of the redox probe. Data obtained from EIS experiments were analysed by fitting the experimental data to an electrical equivalent circuit model using the software FRA 4.9. For AFM studies, high ordered pyrolytic graphite basal plane electrodes (HOPG, Goodfellow Cambridge Limited) were used. Prior to use, the HOPG was exfoliated in order to obtain a clean and atomically flat surface. The atomic force microscope images were performed in an Agilent 5500 microscope with an Olympus cantilevers (RC800PSA, 200_20 mm). Tapping-mode was used to image the N-CD deposits and substrates. In this mode, the cantilever is oscillated at a frequency close to its resonance frequency. ECL experiments were performed using a bipotentiostat/galvanostat (±4 V DC potential range, ±40 mA maximum measurable current) combined with a Si-Photodiode integrated in a electrochemiluminiscence cell (50.0 μL) from DropSens-Metrohm.

2.3 Procedures

2.3.1 N-CD synthesis

A new kind of amine rich carbon nanodots (N-CD) were synthetized following a microwave-assisted procedure. D-Fructose (1.0 mmol) and urea (3.0 mmol) were used as starting carbon and nitrogen sources, respectively. The solids were dissolved in 10.0 mL of distilled water giving rise to a colourless solution. The mixture was heated in a microwave oven for 4 min at 750 W. The initially colourless solution turned brown and finally gave rise to a caramelized dark brown solid. This solid was heated at 60°C for 1 h and subsequently resuspended in 20.0 mL of distilled water

and left overnight at room temperature and protected from light. The N-CD solution was stirred on a plate for 1 h. and then centrifuged for 20 min at 10000 rpm to eliminate possible agglomerated impurities. The brown coloured supernatant was filtered through a nylon mesh of 0.20 μm and finally, dialyzed against distilled water using a dialysis tube for 24 h at room temperature. As-prepared N-CD remained stable in solution at 4°C for several weeks.

2.3.2 N-CD diazonium salt electrografting

N-CD diazotation was performed in an ice bath by mixture of 1.0 ml of a solution containing 12.7 mg/ml of N-CD in 0.5 M HCl and 1.0 mL of 14.5 mM $NaNO_2$. The electrografting was made by adding 80 μL of the N-CD diazonium salt onto carbon electrodes (SPGE and HOPG) and cycling the potential between 0.0 V and +0.8 V at 0.10 V/s to electrochemically reduce in situ generated diazonium salt.

3. Results and discussion

3.1 N-CD synthesis and characterization

In order to obtain CD peripheral enriched in nitrogen containing groups, N-CD were synthetized by a carbonization method microwave-assisted using D-fructose as carbon source and urea as both nitrogen source and passivating agent (following the procedure described in the Experimental Section). The synthesis takes place in two sequential steps: the first one involves the dehydration of the D-fructose, resulting in the nucleation of the CD aromatic core. This nucleation process is evidenced by a change in the colour of the solution, which turns from colourless to brown [31]. The second step involves the carbonization of the carbohydrate, giving rise to the growth of the nanomaterial. At the same time, the increase of the temperature causes the urea decomposition generating ammonia that acts as a catalyst of the carbohydrate carbonization. Urea also acts as a passivating agent of the formed carbon nanodots through the generation of amino groups that act

as capping agents [8, 32]. This passivation step with a nitrogen containing compound may be the responsible of the high stability and the optical properties observed for the as-prepared nitrogen-doped carbon nanodots [33].

The elemental analysis of the synthetized N-CD indicates the following contents: carbon 43.5±0.2%; hydrogen 5.3±0.1%; nitrogen 21.1±0.2% and oxygen 30.1% (calculated by difference). These percentages vary during the first 3 minutes of the synthesis. Afterwards, the elemental analysis gives constant values. According to these results, the synthesis used gives rise to nanoparticles with a high percentage of nitrogen and a molar ratio C/N around 2.4. The C/N ratio confirms the surface enrichment of nitrogen.

Figure 1(a) shows the transmission electron microscopy (TEM) image of as-prepared N-CD. This TEM image suggests that most of purified N-CD are almost spherical with diameter of 5.5 nm and in mono-dispersed populations. The presence of nitrogen functional groups on the surface of each nanoparticle enhances their stability and avoids the presence of aggregates.

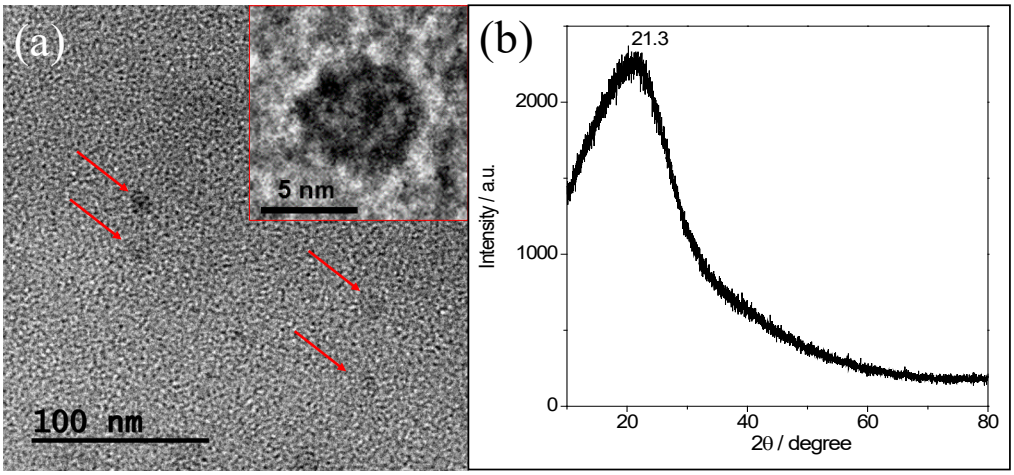

Figure 1 (a) TEM images of the synthetized N-CD. Inset: HR-TEM image of a single N-CD. (b) XRD pattern of N-CD.

The study of individual nanoparticles by HR-TEM (Fig. 1(a), inset) did not show a clearly defined lattice structure suggesting that the purified nanoparticles have a strong percentage of amorphous structure. The X-ray diffraction pattern (XRD) of the N-CD (Fig. 1(b)) showed a very broad peak at 2θ=21.3°, indicating the presence of a nucleus of carbon in amorphous phase. This result agrees well with that observed by HR-TEM [13].

The Fourier transform infrared (FTIR) analysis was carried out to determine the functional groups present on the N-CD surface. The FTIR spectrum of N-CD was compared with the corresponding spectra of the starting compounds (D-fructose and urea). As can be seen in Fig. 2(a), N-CD spectrum depicts a wide band at around 3300 cm^{-1}. This band is ascribed to stretching vibrations of -OH and -NH bonds, suggesting the presence of hydroxyl and amino groups on N-CD surface [34]. Other less intense absorption bands at 1050 cm^{-1} and 1221 cm^{-1} can be assigned to bending and stretching vibrations corresponding to C-O bonds present in carboxyl groups [35]. In summary, FTIR analysis suggests that N-CD synthetized are mainly surrounded by amino, hydroxyl and carboxyl groups. The presence of these polar functional groups explains the good solubility of these nanoparticles in aqueous media, giving rise to pale brown solutions at room temperature. This excellent solubility agrees well with the presence of peripheral charged functional groups. Hence, the zeta potential of N-CD in aqueous solutions (0.06 mg/mL) was determined. As can be seen in Fig. 2(b), the value of the zeta potential was found to be +90.20 mV. This value indicates that the N-CD have a strong positive charge, probably due to the presence of protonated amino groups on the nanoparticle surface. This positive charge avoids nanodots aggregation improving their solubility in aqueous solution [36].

The N-CD optical properties were also explored. For this purpose, we carried out detailed studies by UV-Vis absorption spectroscopy and PL emission by using different excitation wavelengths. The N-CD electronic spectrum (0.10 mg/mL) in aqueous solution shows two absorption bands at 212 nm and 280 nm, as is shown in Fig. 2(c). The band at 212 nm is attributed to transitions π- π* characteristic of the C=C bond of the sp^2 domains corresponding to the aromatic rings present in

the core of the nanodot [37, 38]. The band at 280 nm corresponds to n-π* transitions characteristic of C=O bonds present in the functional groups covalently bound to the outer sp^3 carbons of the nanodot [39]. Besides these two bands, a strong absorption between 300 and 450 nm, without a defined band, is observed. It can be attributed to the different functional groups present at the N-CD surface.

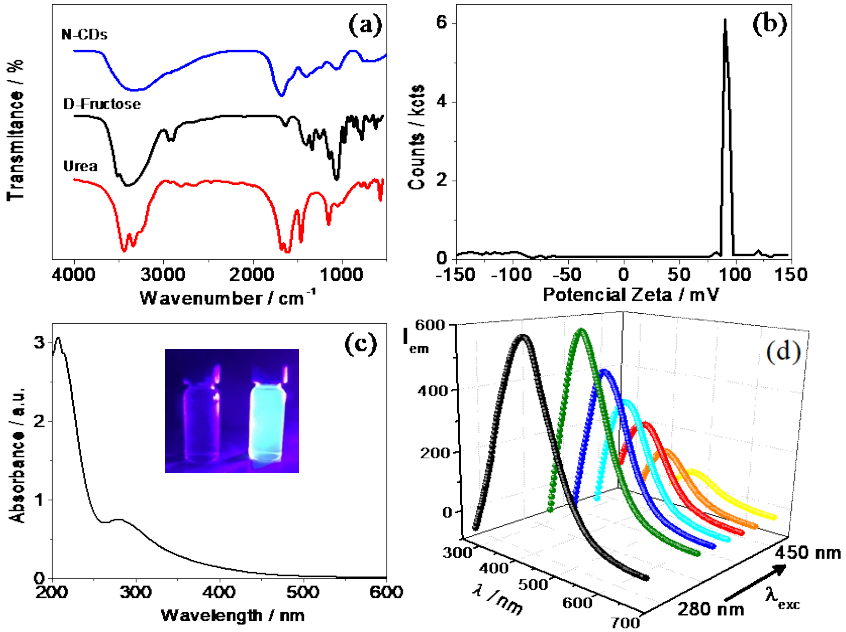

Figure 2 (a) FTIR spectra of D-fructose (black), urea (red) and as-prepared N-CD (blue). (b) Zeta potential of N-CD aqueous solution (0.06 mg/mL). (c) Electronic spectrum and (d) emission spectra, at different excitation wavelengths, of N-CD (0.10 mg/mL) in aqueous solution. Inset of Fig. 2C shows photographs of a mixture of the precursors (left) and N-CD (right) under UV light at 365 nm.

In particular, amino groups present an absorption band at 430 nm due to n-π transitions [38, 40]. The as-prepared N-CD aqueous solutions show a light brown coloration at the ambient light while show blue fluorescence when they are irradiated with a hand-held UV lamp, as can be seen in the inset of Fig. 2(c). As a result, the fluorescence spectrum of the N-CD depicts a maximum of emission at 405 nm when the solution is excited at 280 nm. In a similar way to other dispersions of N-rich carbon nanodots, the as-prepared N-CD fluorescent emission is quite sensitive to

changes in the excitation wavelength (see in Fig. 2(d)). A red shift of the emission wavelength is observed when the excitation wavelength gradually increases from 280 to 450 nm. Concomitant with this bathochromic effect, the emission intensity gradually decreases. This effect is characteristic of CD and is attributed to both, the presence of functional groups attached to their surface and effects of radiation dispersion due to the presence of nanoparticles of different sizes [33, 41]. N-CD fluorescent emission also depends on their concentration (Fig. S-1 in the Supporting Information). The fluorescence intensity of N-CD solutions increases on increasing the concentration from 0.01 to 0.8 mg/mL. However, at concentrations higher than 0.8 mg/mL a drastic decrease of the fluorescence intensity concomitant with a red shift is observed. These changes in fluorescence intensity at high concentrations of N-CD can be attributed to aggregation effects [42].

The estimation of the N-CD quantum yield in aqueous solution gives an idea of the efficiency of the fluorophore as photoluminescent material, since it allows establishing the relationship between the luminescent particles and the total number of particles. The synthetized N-CD quantum yield was calculated using as standard a quinine sulphate solution in 0.1 M H_2SO_4. Experiments were carried out using an excitation wavelength (λ_{ex}=280 nm) and the quantum yields were determined using the following equation:

$$\phi_x = \phi_{st}\left(\frac{I_x}{I_{st}}\right)\left(\frac{A_{st}}{A_x}\right)\left(\frac{\eta_x^2}{\eta_{st}^2}\right)$$

where φ represents the quantum yield, I is the fluorescence intensities at the corresponding excitation wavelength, A is the absorbance measured and η are the refractive indexes of the solvent. The subscript x refers to the sample of N-CD while the subscript st refers to the solutions of the standard. Under these conditions, the quantum yield of the as-prepared N-CD was found to be around 1.5%. This low value can be attributed to the high nitrogen content of these N-CD, that

can reduce the effective defects of the surface leading to a drastic reduction of the efficiency of the fluorescent emission [42].

3.2 Electrografting of the N-CD onto an HOPG electrode

According to the characterization experiments described above, we can affirm that as we expected, the microwave-assisted synthesis of carbon nanodots using D-fructose and urea as starting materials produces fluorescent carbon nanodots peripheral enriched in nitrogen functional groups. In addition to the chemical properties that these functional groups may confer to these N- CD [27, 43], they can be employed to modify the nanomaterial with specific functionalities by post-synthesis reactions, endowing it with interesting properties or allowing its covalent immobilization on different substrates. Hence, in a second step, we proceed to explore the presence of aromatic amines on the N-CD surface and its transformation in highly reactive aryldiazonium salt by reaction with nitrite ion in acid media. The reactivity of the aryldiazonium groups will open a wide range of potential application of these diazotized carbon nanodots ($\oplus N_2$-CD), in particular its covalent attachment to conductive surfaces *via* electrografting. Taking this in mind, synthetized N-CD were diazotized in 0.5 M HCl at 4°C in the presence of sodium nitrite, as described in the Experimental Section. Aliquots of this solution were placed on the surface of SPGE or HOPG. Then, the potential was cycled between 0.0 V and -0.8 V several times. Figure 3(b) shows the cyclic voltammograms recorded using SPGE (N-CD/SPGE). It can be seen that during the first cathodic scan a reduction process with a clearly defined cathodic peak at -0.55 V appears. This reduction is irreversible (no anodic process is detected in the corresponding anodic scan) and is ascribed to the reduction of aryldiazonium groups ($\oplus N_2$-CD). This electrochemical reduction gives rise to highly reactive nucleophilic aryl groups, which are quickly electrografted on the electrode surface as depicted in Figure 4. In the successive potential scans, a gradual reduction of the cathodic peak current is observed. This behaviour is characteristic of

electrografting processes [44-47] and it can be explained if one takes into account that, once the first monolayer has been formed, the nanoparticles attached to the electrode surface exert a blocking effect that prevents the incorporation of new nanoparticles. Control experiments were carried out in the same conditions, but using non-diazotized N-CD solutions (Fig. 3(a)). In this case, the irreversible reduction process is not observed. These results confirm that the as-prepared N-CD have aromatic amines on their surface that allows their immobilization by electrografting.

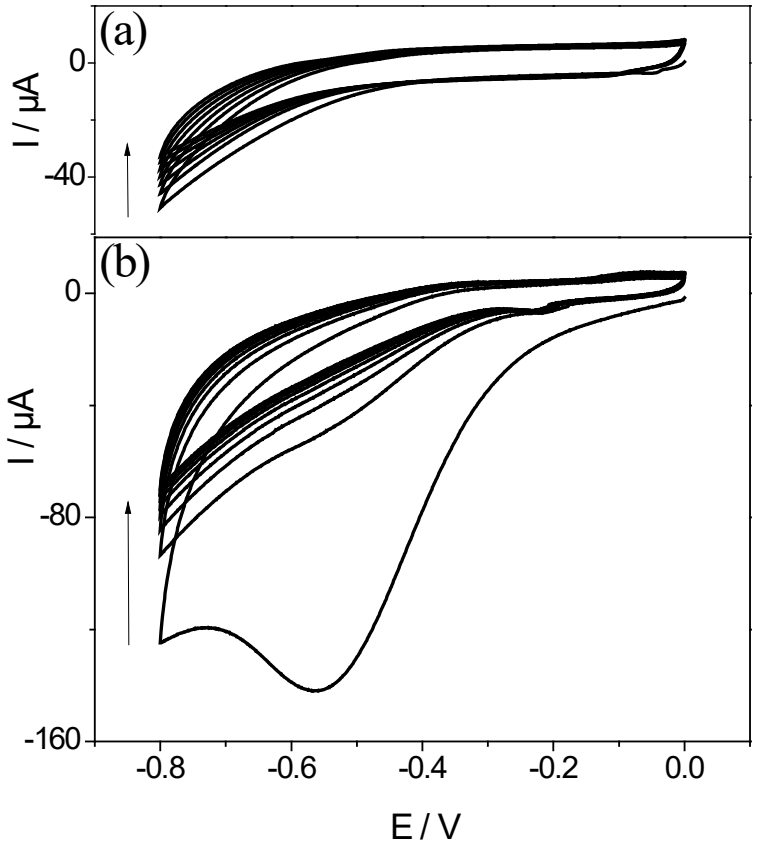

Figure 3 (a) Cyclic voltammograms of 6.3 mg/mL N-CD in 0.5 M HCl in the absence of $NaNO_2$ at a SPGE. (b) Cyclic voltammograms of Diazotized N-CD electrografting prepared as indicated in the Experimental Section at SPGEs. 10 consecutive scans were performed. Scan rate 0.10 V/s.

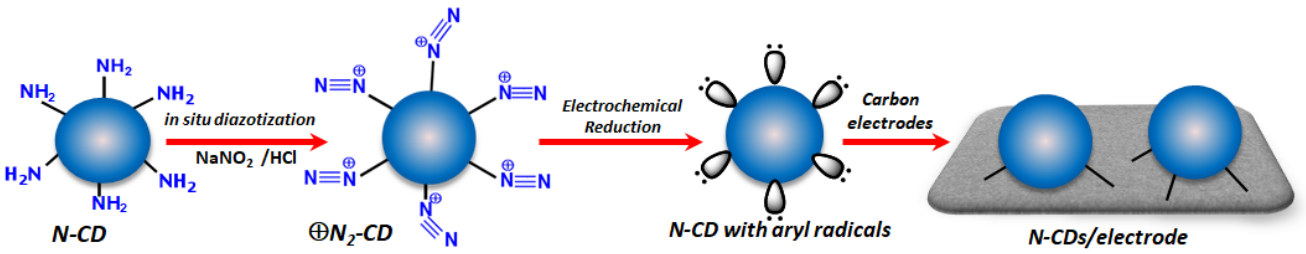

Figure 4 Diazotized N-CD electrografting on carbon electrodes.

3.3 Characterization of the electrografted electrode

AFM measurements were carried out to confirm the presence of electrografted N-CD onto the carbon electrode surfaces and to study the morphology and distribution of the immobilized nanostructures. These AFM studies were carried out onto carbon electrodes with a flat surface, such as the basal plane HOPG. Figure 5(a) shows a 2.1 μm wide image of a bare basal plane HOPG. The image was taken in tapping-mode and shows the typical arrangement of the basal plane HOPG substrates characterized by the presence of wide flat terraces and steps (Fig. 5(a), green line) of approximately 2-3 Å in height. In the terraces, a surface with an extremely smoother granulate is observed, in which the triangular facet arrangements characteristic of the HOPG are also visible. When this surface is imaged in contact mode on atomic scale, we observe the atomic arrangement corresponding to the basal surface plane HOPG (data not show). It should be noted that the height range of Fig. 5(a) has been adjusted to be the same as the range used in the AFM images corresponding to the modified HOPG surfaces with the electrografted N-CD (N-CD/HOPG). Figure 5(b) shows a 4.0 μm wide AFM image of a HOPG surface modified by electrografting with N-CD. At this level of magnification, it is observed that the surface of the HOPG is homogeneously covered with granular structures of spherical shape, small size and randomly distributed. On the other hand, it should be noted that the triangular facet arrangements of the HOPG can still be observed in spite of the N-CD incorporation to the surface. Even the linear boundaries between some of the different facets are marked by the presence of

electrografted nanodots that are arranged following the line of the border between facets. This linear arrangement is more noticeable at a higher level of magnification (960 nm wide; Fig. 5(c)) suggesting that the electrografting process is initially favoured on steps and borders between facets of HOPG. This level of magnification makes possible to observe the presence of areas in which, together with individual nanodots, they appear aggregated in the form of collar beads, which suggests that the electrografting process can also give rise to lateral interactions between the N-CD.

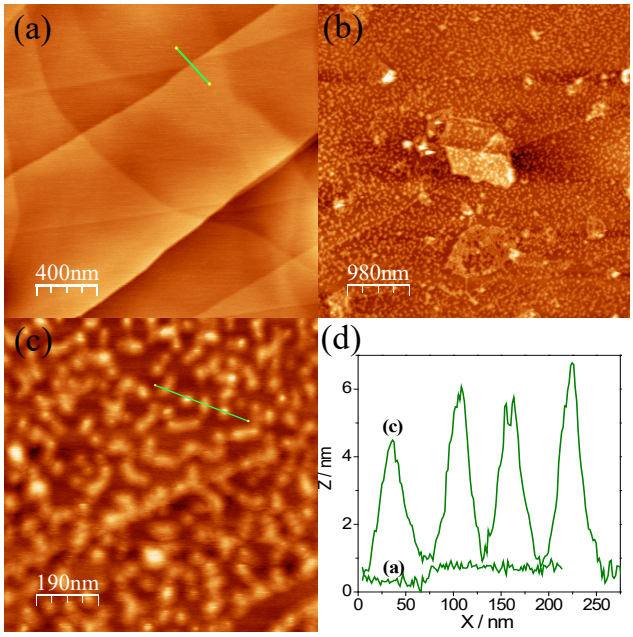

Figure 5 AFM images of bare HOPG (a) and electrografted N-CD onto basal plane HOPG surface (b and c). (d) Topographic profiles of the green lines drawn in (a) and (c).

The topography of the surface of HOPG modified with N-CD was studied using the tapping-mode at a constant force and sweeping the curve along the green line shown in Fig. 5(c). The topographic profile obtained (Fig. 5(d)) shows very regular nanostructures comprised between 15 and 20 nm in diameter. Although this value is higher than that estimated by TEM, it can be explained by deconvolution tip effects. Moreover, it cannot be determined whether these structures correspond to individual and discretely separated N-CD or to aggregates formed by the interaction between

several N-CD. In any case, the structures obtained are fairly uniform in size along the entire surface. The estimated average high of 5.8±0.8 nm would correspond with a monolayer of N-CD. The stability of the resulting N-CD/HOPG modified electrodes was evaluated. For this purpose, N-CD/HOPG modified electrodes were immersed in 0.1 M NaOH solution and sonicated in an ultrasonic bath for 15 min. Then they were thoroughly washed with distilled water. After the treatment, the electrode topography was imaged using the tapping-mode AFM. The N-CD/HOPG surface appears still covered with rounded features with similar arrangements to those depicted in Fig. 5(b) and 5(c) (Fig. S-2). These results confirm that modification of carbon electrodes by diazotized N-CD electrografting gives rise to highly covered and stable surfaces.

The electrochemical impedance spectroscopy is an electrochemical technique that allows us to study the interfacial properties of a modified conductive surface. We have used this technique to study the changes produced in electrochemical properties such as capacitance and charge transfer resistance at SPGE, after modification with electrografted N-CD. Figure 6 shows Nyquist plots obtained when SPGEs (1) and N-CD/SPGEs (2) are subjected to impedance analysis in solutions containing the redox system $[Fe(CN)_6]^{3-/4-}$ in 0.1 M acetic acid/acetate buffer (pH=5). Two clearly differentiated regions are observed. At high frequencies, we can see semicircular representations from which the resistance to charge transfer (R_{CT}) was estimated. However, at low frequencies, representations are linear and ascribed to the diffusion control of the electrochemical process. The experimental data were fit according to the Randles equivalent circuit included in Fig. 6, resulting in the solid lines presented in the figure. The experimental results and the fit for SPGEs and N-CD/SPGEs are listed in Table S-1. After the modification of SPGEs by diazotized N-CD electrografting the charge transfer resistance decreased from 550 Ω to 216 Ω, suggesting that the conductivity of this surface is higher than the bare SPGE. Hence, based on both the better conductivity and higher relative active surface, N-CD/SPGEs will be an interesting electrochemical platform for (bio)sensor applications.

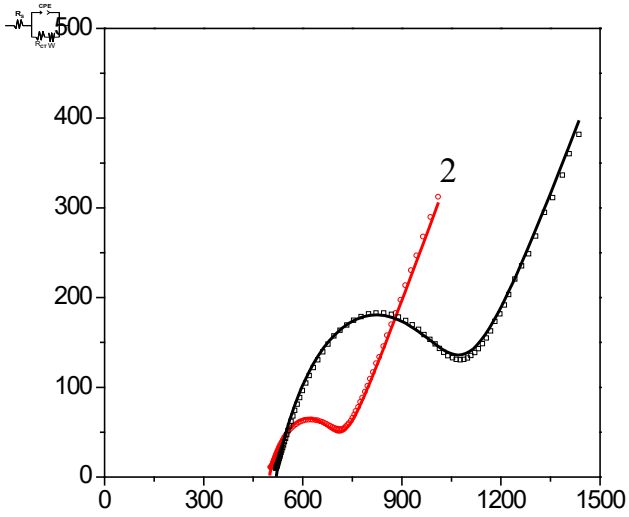

Figure 6 Nyquist diagrams obtained in 0.1 M acetic acid/acetate buffer (pH=5) in the presence of 10 mM $K_3Fe(CN)_6$/10 mM $K_4Fe(CN)_6$ for bare SPGE (1) and N-CD/SPGEs (2). Solid lines correspond to the fitting of the experimental data. Inset: Electrical equivalent circuit.

3.4 The N-CD electrografted electrode as an electrochemiluminescent sensing platform

Based on results described above, we have studied the potential application of developed N-CD nanostructured electrodes as electrochemiluminescent sensing platforms. CD have been previously employed in electrochemiluminescence sensing. Various coreactants and nanomaterials have been combined with CD as signal amplification agents to enhance the performance of sensors [48, 49]. Taking into account these previous works, we wanted to know if N-CD/SPGEs are able to amplify the ECL response of the $[Ru(bpy)_3]^{2+/3+}$, which is a well-known photoluminiscent redox system, in order to develop improved ECL sensor platforms.

As a proof of concept, we studied the determination of taurine following the ECL process depicted in the scheme of Fig. 7(a) where the $[Ru(bpy)_3]^{2+}$ is used as luminophore. Taurine (2-amino ethanesulfonic acid) is a non-essential amino acid that plays an important role in many functions and biological processes [50]. Its detection is of great importance for clinical diagnostics and quality control in the manufacturing industry.

ECL is an unique and sensitive analytical method that can be employed for determination of taurine, since it has an amine [51]. Therefore, it can be both coreactant and analyte simultaneously in an ECL assay (see Fig. 7(a)). As a starting point, the cyclic voltammetric behaviour of a solution of $[Ru(bpy)_3]^{2+}$ (2.0 mM) containing 20 mM of taurine was studied at both bare SPGE and N-CD/SPGEs (Fig. S-3). At bare SPGE the voltammetric wave ascribed to the redox couple Ru^{3+}/Ru^{2+} is observed. However, at N-CD/SPGEs there is an increase in the anodic current concomitant with a significant decrease in the current of the cathodic reverse scan, which is characteristic of an electrocatalytic effect. This effect is reflected in the ECL signal in presence of taurine [52]. Figure 7(b), black line depicts the ECL signal plotted *vs* time obtained when N-CD/SPGEs are immersed in solutions containing 2.0 mM $[Ru(bpy)_3]^{2+}$ and 20 mM of taurine in 0.1 M phosphate buffer (pH=8.0). The potential was cycled several times between 0.0 V and +1.3 V at 0.05 V/s. As can be seen the ECL emission is stable and around three-times higher than that obtained under the same conditions at unmodified SPGEs, used as control (Fig. 7(b), red line). According with these results, N-CD electrografting on carbon surfaces gives rise to very stable N-CD modified electrode surfaces, with improved conductivity and a much more sensitive ECL response. Moreover, the ECL signal increases linearly on increasing the concentration of taurine. Hence, it can be employed as an improved taurine sensor.

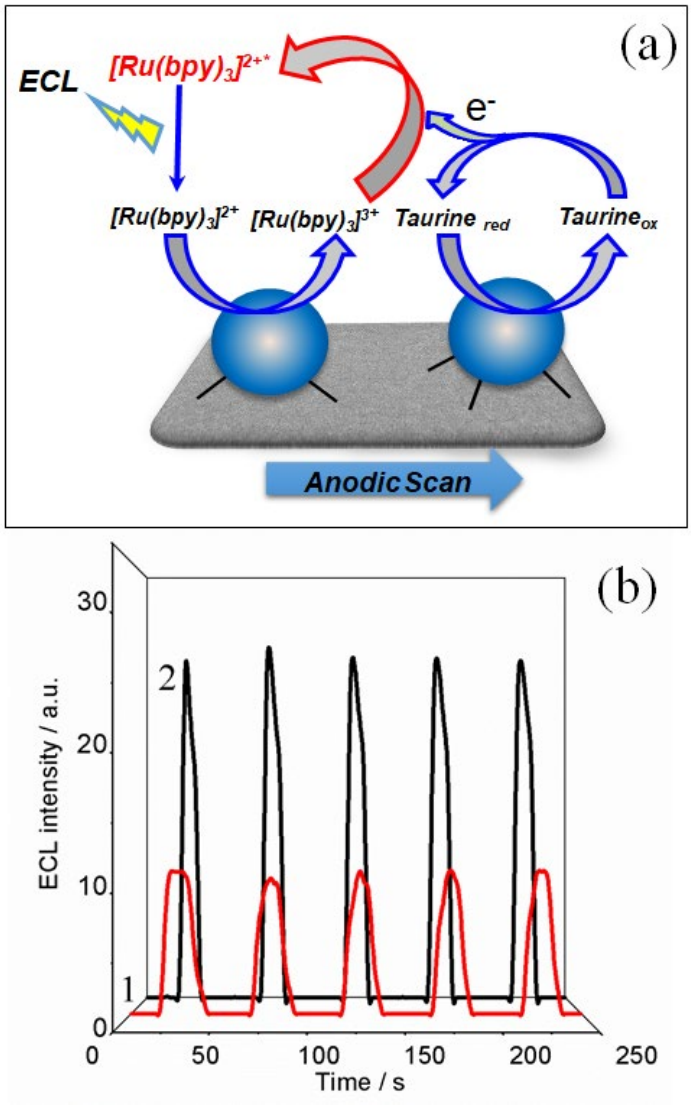

Figure 7 (a) Schematic representation of the ECL process. (b) ECL response at a bare SPGE (1) or N-CD/SPGE (2) measured under consecutive cyclic potential scans in 0.1 M phosphate buffer (pH=8.0) containing 2.0 mM $[Ru(bpy)_3]^{2+}$ and 20 mM taurine. Scan rate: v=0.05 V/s.

Calibration plots obtained for quantification of taurine by ECL at a N-CD/SPGE and a bare SPGE are depicted in the Figure S4. Aliquots were added in triplicate at concentrations of taurine from 250.0 µM to 1000 µM. Plots of ECL signal vs taurine concentration show a linear behavior up to 1000 µM, from whose slopes sensitivities of 2.20×10^{-4} and 7.40×10^{-4} μM^{-1} were calculated for bare SPGE and N-CD/SPGE, respectively. The sensitivity increases three times when N-CD modified electrodes are employed compared with the bare electrode. Detection and quantification

limits of 37.8 and 126 μM, respectively, were estimated from the standard deviation of the background current (3 Sb/m and 10 Sb/m, respectively).

The relative standard deviation of the response of three different biosensors prepared in the same manner was employed to evaluate the reproducibility of the biosensor. It was found to be of 3.8 %, which implies that the method has a good precision.

The ECL response at N-CD/SPGE measured under consecutive cyclic potential scans from 0.0 to +1.3 V during 2500 s was employed to test the stability of the platform. It was found that after 50 cycles, the platform kept 86 % of the initial response.

The storage stability was also evaluated by measuring the response for 10 days. N-CD/SPGEs were stored. After this period of storage, the ECL sensor lost only 3 % of its initial response. These results confirm that the immobilization N-CDs on carbon electrodes by electrografting gives rise to a very stable platform that retains its electrochemiluminescent properties.

4. Conclusions

The microwave-assisted synthesis of N-doped carbon nanodots (N-CD) using D-fructose and urea as starting materials produces nanostructures with a high content of nitrogen, close to 21%. These N-CD present a nucleus with a predominantly amorphous structure. This core is surrounded by peripheral functional groups, such as amino, carboxyl and hydroxyl among others. Due to the presence of these peripheral charged functionalities, the water solutions of these N-CD are stable, showing a pale brown colour. When these CD are irradiated with ultraviolet light (365 nm) they show a powerful blue luminescence. Some of the peripheral amino groups present in the N-CD are aromatic and therefore susceptible to be transformed by reaction with nitrite in acid medium to the corresponding diazonium salts. Diazotized N-CD can be electrografted onto the surface of carbon electrodes, confirming the presence of aromatic amines and generating a stable nano-hybrid surface that shows a higher electrical conductivity, compared with the unmodified surface, and a potent and persistent electrocatalytic effect towards the oxidation of $[Ru(bpy)_3]^{2+}$. Taking

advantage of these properties, we have employed N-CD/SPGE as a sensing platforms for the sensitive determination of taurine, that acts as coreactant in the ECL associated to ruthenium complexes.

Acknowledgments

This work has been supported by the Spanish Ministerio de Ciencia, Innovación y Universidades through projects CTQ2017-84309-C2-1-R and RED2018-102412-T, and Comunidad Autónoma de Madrid (S2018/NMT-4349 TRANSNANOAVANSENS-CM Program and 2017-T1/BIO-5435 Atracción de Talento Project). The authors thank Professor Hector Abruña the critical review of this work.

References

[1]Sinha, A.;Dhanjai;Jain, R.;Zhao, H.;Karolia, P.; Jadon, N. Voltammetric sensing based on the use of advanced carbonaceous nanomaterials: a review. *Microchimica Acta* **2018**, *185*, 89.

[2]Antonietti, M.;Lopez-Salas, N.; Primo, A. Adjusting the Structure and Electronic Properties of Carbons for Metal-Free Carbocatalysis of Organic Transformations. *Advanced Materials* **2019**, *31*, 1805719.

[3]Dey, S.;Chithaiah, P.;Belawadi, S.;Biswas, K.; Rao, C. N. R. New methods of synthesis and varied properties of carbon quantum dots with high nitrogen content. *Journal of Materials Research* **2014**, *29*, 383-391.

[4]Li, H.;Chen, L.;Wu, H.;He, H.; Jin, Y. Ionic Liquid-Functionalized Fluorescent Carbon Nanodots and Their Applications in Electrocatalysis, Biosensing, and Cell Imaging. *Langmuir* **2014**, *30*, 15016-15021.

[5]Bao, L.;Zhang, Z.-L.;Tian, Z.-Q.;Zhang, L.;Liu, C.;Lin, Y.;Qi, B.; Pang, D.-W. Electrochemical Tuning of Luminescent Carbon Nanodots: From Preparation to Luminescence Mechanism. *Advanced Materials* **2011**, *23*, 5801-5806.

[6]Hsu, P.-C.; Chang, H.-T. Synthesis of high-quality carbon nanodots from hydrophilic compounds: role of functional groups. *Chemical Communications* **2012**, *48*, 3984-3986.

[7]Zhang, B.;Liu, C.-y.; Liu, Y. A Novel One-Step Approach to Synthesize Fluorescent Carbon Nanoparticles. *European Journal of Inorganic Chemistry* **2010**, *2010*, 4411-4414.

[8]Wang, X.;Qu, K.;Xu, B.;Ren, J.; Qu, X. Microwave assisted one-step green synthesis of cell-permeable multicolor photoluminescent carbon dots without surface passivation reagents. *Journal of Materials Chemistry* **2011**, *21*, 2445-2450.

[9]Anwar, S.;Ding, H.;Xu, M.;Hu, X.;Li, Z.;Wang, J.;Liu, L.;Jiang, L.;Wang, D.;Dong, C.;Yan, M.;Wang, Q.; Bi, H. Recent Advances in Synthesis, Optical Properties, and Biomedical Applications of Carbon Dots. *ACS Applied Bio Materials* **2019**, *2*, 2317-2338.

[10]Campuzano, S.;Yáñez-Sedeño, P.; Pingarrón, M. J. Carbon Dots and Graphene Quantum Dots in Electrochemical Biosensing. *Nanomaterials* **2019**, *9*.

[11]Qi, B.-P.;Bao, L.;Zhang, Z.-L.; Pang, D.-W. Electrochemical Methods to Study Photoluminescent Carbon Nanodots: Preparation, Photoluminescence Mechanism and Sensing. *ACS Applied Materials & Interfaces* **2016**, *8*, 28372-28382.

[12]Pirsaheb, M.;Mohammadi, S.; Salimi, A. Current advances of carbon dots based biosensors for tumor marker detection, cancer cells analysis and bioimaging. *TrAC Trends in Analytical Chemistry* **2019**, *115*, 83-99.

[13]Baker, S. N.; Baker, G. A. Luminescent Carbon Nanodots: Emergent Nanolights. *Angewandte Chemie International Edition* **2010**, *49*, 6726-6744.

[14]Zheng, B.;Liu, T.;Paau, M. C.;Wang, M.;Liu, Y.;Liu, L.;Wu, C.;Du, J.;Xiao, D.; Choi, M. M. F. One pot selective synthesis of water and organic soluble carbon dots with green fluorescence emission. *RSC Advances* **2015**, *5*, 11667-11675.

[15] Li, H.;He, X.;Kang, Z.;Huang, H.;Liu, Y.;Liu, J.;Lian, S.;Tsang, C. H. A.;Yang, X.; Lee, S.-T. Water-Soluble Fluorescent Carbon Quantum Dots and Photocatalyst Design. *Angewandte Chemie International Edition* **2010**, *49*, 4430-4434.

[16] Liu, R.;Wu, D.;Liu, S.;Koynov, K.;Knoll, W.; Li, Q. An Aqueous Route to Multicolor Photoluminescent Carbon Dots Using Silica Spheres as Carriers. *Angewandte Chemie International Edition* **2009**, *48*, 4598-4601.

[17] Lingam, K.;Podila, R.;Qian, H.;Serkiz, S.; Rao, A. M. Evidence for Edge-State Photoluminescence in Graphene Quantum Dots. *Advanced Functional Materials* **2013**, *23*, 5062-5065.

[18] Sun, Y.;Wang, S.;Li, C.;Luo, P.;Tao, L.;Wei, Y.; Shi, G. Large scale preparation of graphene quantum dots from graphite with tunable fluorescence properties. *Physical Chemistry Chemical Physics* **2013**, *15*, 9907-9913.

[19] Li, H.;Kang, Z.;Liu, Y.; Lee, S.-T. Carbon nanodots: synthesis, properties and applications. *Journal of Materials Chemistry* **2012**, *22*, 24230-24253.

[20] Yu, D.;Zhang, Q.; Dai, L. Highly Efficient Metal-Free Growth of Nitrogen-Doped Single-Walled Carbon Nanotubes on Plasma-Etched Substrates for Oxygen Reduction. *Journal of the American Chemical Society* **2010**, *132*, 15127-15129.

[21] Gong, K.;Du, F.;Xia, Z.;Durstock, M.; Dai, L. Nitrogen-Doped Carbon Nanotube Arrays with High Electrocatalytic Activity for Oxygen Reduction. *Science* **2009**, *323*, 760-764.

[22] Qu, L.;Liu, Y.;Baek, J.-B.; Dai, L. Nitrogen-Doped Graphene as Efficient Metal-Free Electrocatalyst for Oxygen Reduction in Fuel Cells. *ACS Nano* **2010**, *4*, 1321-1326.

[23] Jeong, H. M.;Lee, J. W.;Shin, W. H.;Choi, Y. J.;Shin, H. J.;Kang, J. K.; Choi, J. W. Nitrogen-Doped Graphene for High-Performance Ultracapacitors and the Importance of Nitrogen-Doped Sites at Basal Planes. *Nano Letters* **2011**, *11*, 2472-2477.

[24] Gopalakrishnan, K.;Moses, K.;Govindaraj, A.; Rao, C. N. R. Supercapacitors based on nitrogen-doped reduced graphene oxide and borocarbonitrides. *Solid State Communications* **2013**, *175-176*, 43-50.

[25] Wu, Q.;Xu, Y.;Yao, Z.;Liu, A.; Shi, G. Supercapacitors Based on Flexible Graphene/Polyaniline Nanofiber Composite Films. *ACS Nano* **2010**, *4*, 1963-1970.

[26] Zhang, Y.-Q.;Ma, D.-K.;Zhuang, Y.;Zhang, X.;Chen, W.;Hong, L.-L.;Yan, Q.-X.;Yu, K.; Huang, S.-M. One-pot synthesis of N-doped carbon dots with tunable luminescence properties. *Journal of Materials Chemistry* **2012**, *22*, 16714-16718.

[27] Hu, C.;Liu, Y.;Yang, Y.;Cui, J.;Huang, Z.;Wang, Y.;Yang, L.;Wang, H.;Xiao, Y.; Rong, J. One-step preparation of nitrogen-doped graphene quantum dots from oxidized debris of graphene oxide. *Journal of Materials Chemistry B* **2013**, *1*, 39-42.

[28] Ma, Z.;Ming, H.;Huang, H.;Liu, Y.; Kang, Z. One-step ultrasonic synthesis of fluorescent N-doped carbon dots from glucose and their visible-light sensitive photocatalytic ability. *New Journal of Chemistry* **2012**, *36*, 861-864.

[29] Xu, Y.;Wu, M.;Liu, Y.;Feng, X.-Z.;Yin, X.-B.;He, X.-W.; Zhang, Y.-K. Nitrogen-Doped Carbon Dots: A Facile and General Preparation Method, Photoluminescence Investigation, and Imaging Applications. *Chemistry – A European Journal* **2013**, *19*, 2276-2283.

[30] Delamar, M.;Hitmi, R.;Pinson, J.; Saveant, J. M. Covalent modification of carbon surfaces by grafting of functionalized aryl radicals produced from electrochemical reduction of diazonium salts. *Journal of the American Chemical Society* **1992**, *114*, 5883-5884.

[31] Yang, X.;Yang, X.;Li, Z.;Li, S.;Han, Y.;Chen, Y.;Bu, X.;Su, C.;Xu, H.;Jiang, Y.; Lin, Q. Photoluminescent carbon dots synthesized by microwave treatment for selective image of cancer cells. *Journal of Colloid and Interface Science* **2015**, *456*, 1-6.

[32] Yu, S. H.;Cui, X. J.;Li, L. L.;Li, K.;Yu, B.;Antonietti, M.; Cölfen, H. From Starch to Metal/Carbon Hybrid Nanostructures: Hydrothermal Metal-Catalyzed Carbonization. *Advanced Materials* **2004**, *16*, 1636-1640.

[33] Zhu, S.;Meng, Q.;Wang, L.;Zhang, J.;Song, Y.;Jin, H.;Zhang, K.;Sun, H.;Wang, H.; Yang, B. Highly Photoluminescent Carbon Dots for Multicolor Patterning, Sensors, and Bioimaging. *Angewandte Chemie International Edition* **2013**, *52*, 3953-3957.

[34] Niu, J.;Gao, H.;Wang, L.;Xin, S.;Zhang, G.;Wang, Q.;Guo, L.;Liu, W.;Gao, X.; Wang, Y. Facile synthesis and optical properties of nitrogen-doped carbon dots. *New Journal of Chemistry* **2014**, *38*, 1522-1527.

[35] Hu, S.-L.;Niu, K.-Y.;Sun, J.;Yang, J.;Zhao, N.-Q.; Du, X.-W. One-step synthesis of fluorescent carbon nanoparticles by laser irradiation. *Journal of Materials Chemistry* **2009**, *19*, 484-488.

[36] Qu, S.;Wang, X.;Lu, Q.;Liu, X.; Wang, L. A Biocompatible Fluorescent Ink Based on Water-Soluble Luminescent Carbon Nanodots. *Angewandte Chemie International Edition* **2012**, *51*, 12215-12218.

[37] Shen, C.;Sun, Y.;Wang, J.; Lu, Y. Facile route to highly photoluminescent carbon nanodots for ion detection, pH sensors and bioimaging. *Nanoscale* **2014**, *6*, 9139-9147.

[38] Sahu, S.;Behera, B.;Maiti, T. K.; Mohapatra, S. Simple one-step synthesis of highly luminescent carbon dots from orange juice: application as excellent bio-imaging agents. *Chemical Communications* **2012**, *48*, 8835-8837.

[39] Qu, D.;Sun, Z.;Zheng, M.;Li, J.;Zhang, Y.;Zhang, G.;Zhao, H.;Liu, X.; Xie, Z. Three Colors Emission from S,N Co-doped Graphene Quantum Dots for Visible Light H2 Production and Bioimaging. *Advanced Optical Materials* **2015**, *3*, 360-367.

[40] Qu, D.;Zheng, M.;Li, J.;Xie, Z.; Sun, Z. Tailoring color emissions from N-doped graphene quantum dots for bioimaging applications. *Light: Science &Amp; Applications* **2015**, *4*, e364.

[41] Wang, C.;Xu, Z.;Cheng, H.;Lin, H.;Humphrey, M. G.; Zhang, C. A hydrothermal route to water-stable luminescent carbon dots as nanosensors for pH and temperature. *Carbon* **2015**, *82*, 87-95.

[42] Niu, Q.;Gao, K.;Lin, Z.; Wu, W. Amine-capped carbon dots as a nanosensor for sensitive and selective detection of picric acid in aqueous solution via electrostatic interaction. *Analytical Methods* **2013**, *5*, 6228-6233.

[43] Kim, T. H.;Ho, H. W.;Brown, C. L.;Cresswell, S. L.; Li, Q. Amine-rich carbon nanodots as a fluorescence probe for methamphetamine precursors. *Analytical Methods* **2015**, *7*, 6869-6876.

[44] Pinson, J.; Podvorica, F. Attachment of organic layers to conductive or semiconductive surfaces by reduction of diazonium salts. *Chemical Society Reviews* **2005**, *34*, 429-439.

[45] Revenga-Parra, M.; Gómez-Anquela, C.; García-Mendiola, T.;Gonzalez, E.;Pariente, F.; Lorenzo, E. Grafted Azure A modified electrodes as disposable β-nicotinamide adenine dinucleotide sensors. *Analytica Chimica Acta* **2012**, *747*, 84-91.

[46] Gutiérrez-Sánchez, C.;Jia, W.;Beyl, Y.;Pita, M.;Schuhmann, W.;De Lacey, A. L.; Stoica, L. Enhanced direct electron transfer between laccase and hierarchical carbon microfibers/carbon nanotubes composite electrodes. Comparison of three enzyme immobilization methods. *Electrochimica Acta* **2012**, *82*, 218-223.

[47] Rüdiger, O.;Abad, J. M.;Hatchikian, E. C.;Fernandez, V. M.; De Lacey, A. L. Oriented Immobilization of Desulfovibrio gigas Hydrogenase onto Carbon Electrodes by Covalent Bonds for Nonmediated Oxidation of H2. *Journal of the American Chemical Society* **2005**, *127*, 16008-16009.

[48] Yang, S.;Liang, J.;Luo, S.;Liu, C.; Tang, Y. Supersensitive Detection of Chlorinated Phenols by Multiple Amplification Electrochemiluminescence Sensing Based on Carbon Quantum Dots/Graphene. *Analytical Chemistry* **2013**, *85*, 7720-7725.

[49] Li, S.;Luo, J.;Yang, X.;Wan, Y.; Liu, C. A novel immunosensor for squamous cell carcinoma antigen determination based on CdTe@Carbon dots nanocomposite electrochemiluminescence resonance energy transfer. *Sensors and Actuators B: Chemical* **2014**, *197*, 43-49.

[50] Huxtable, R. J. Physiological actions of taurine. *Physiological Reviews* **1992**, *72*, 101-163.

[51] Guerrero-Esteban, T.; Gutiérrez-Sánchez, C.; Revenga-Parra, M.;Pau, J. L.;Pariente, F.; Lorenzo, E. Enhanced electrochemiluminescence by ZnO nanowires for taurine determination. *Talanta* **2019**, *204*, 63-69.

[52] Miao, W.;Choi, J.-P.; Bard, A. J. Electrogenerated Chemiluminescence 69: The Tris(2,2‘-bipyridine)ruthenium(II), (Ru(bpy)32+)/Tri-n-propylamine (TPrA) System RevisitedA New Route Involving TPrA•+ Cation Radicals. *Journal of the American Chemical Society* **2002**, *124*, 14478-14485.